

Electron Momentum Density in Nickel (Ni)

Abdul Hadi M .Ghaleb^{*}, Fareed M. Mohammed^{**}, Muataz A. Majeed^{***}, Mohammad N. Mohammed^{**}, Nawras S. Mohammed^{**},

^{*} Department of physics/College of Science/U.O.Kirkuk-IRAQ

^{**} Department of physics/College of Science/U.O.Tikrit-IRAQ

^{***} Ministry of Education /Salahdeen Education Directorate -IRAQ

Abstract

In this paper, Compton profile of (Ni) was Calculated by employing both the renormalized-free atom(RFA) model and free electron(FE) model setting several configurations in subset (3d-4s). The results were compared with recent data ,It shows that the RFA calculation in(3d^{8.8}-4s^{1.2}) gives a better agreement with experiment.The calculated data used for the first time also to compute the cohesive energy of Nickle and compared it with available data. The Band structure and Density of state of Nickel crystals(DFT-LDA) also calculated by using code Quantum wise.

Keywords: Compton profile,Electron momentum density, Cohesive energy, Band structure, Density of state.

Introduction

Nickel is the silvery-white. Hard ,malleable, and ductile metal. It is of the Iron group and it takes on a high polish. It is a fairly good conductor of heat and electricity. In its familiar compounds nickel is bivalent, although it assumes other valence. It also forms a number of complex compounds. Most nickel compounds are blue or green.Nickel dissolves slowly in dilute acids but , Like iron , becomes passive when treated with nitric acids. Finely divided nickel adsorbs hydrogen[1-2]. In the last decade Compton scattering has been recognized as a powerful tool to study electron structure in light and medium transition metals [3-6], experimental results were predicted reasonably well at medium and high-momentum ($P_z > 3.0$ a.u) by the free atom profiles. In the low momentum region more refined calculation employing both the band structure as well as simple renormalized free atom (RFA) models can explain the Compton line shapes. Among 3d metals, very little work has been reported on Ni. The first Compton profile measurement on polycrystalline Ni and observed that the measured values were much flatter than the convoluted free atom values at low momenta[7]. The Compton Profile of Ni were calculated by using spin-polarized self-consistent LCGO band-structure method within the local-density-functional theory[8]. The electronic properties and Compton Profile of Zn and Cd were reported by Brener et al[9]. Electron momentum density and X-ray Structure Factors of Copper using Compton spectrometer Am²⁴¹[10].First experimental Compton profile for (Ni) reported by Paakkari et al [11].It is known that the Compton profile, $J(p_z)$, can provide information about the projection of electronic momentum distribution on the scattering wave vector [12]. Within the impulse approximation, $J(p_z)$ is given by:

$$J(p_z) = \iint \rho(\vec{p}) dp_x dp_y \quad (1)$$

Where p_x and p_y are the momentum components in x and y directions while the z direction is parallel to the resultant of the incident and scattered wave vectors, $\rho(\vec{p})$ momentum density [13]. In all these studies the electron momentum, is p_z expressed in atomic units (a.u.) where $e = \hbar = m = 1, c = 137$ and 1 a.u. of momentum = 1.993×10^{-24} kg . m/s. In §2 we present the details of theoretical calculation . In §3 and 4 described the result and discussion, conclusions. Objective of the study is due to the shortage of refine calculation of electronic momentum density (Ni). In determining these areas, the contributions of (1s) electrons were taken up to 6 a.u. for Ni because beyond these values the recoil energy becomes smaller than the corresponding K-shell binding energy [14].

Calculation

2-1 Renormalized – Free-Atom (RFA) model:

The renormalized - atom approach was the firstly to be used by [15]. In the RFA model one starts with the free -atom wave function, truncates them at the Wigner-Sites (WS) Sphere and renormalizes the wave function to one within this Sphere to preserve charge neutrality .

For bcc metals, the Compton profile for 4s electrons, can be written by as [16]:

$$J_{4s}(P_z) = 4\pi \sum_{n=0}^{\infty} |\Psi_0^c(K_n)|^2 G_n(p_z) \quad (2)$$

Where K_n is a reciprocal lattice vector and p_z the projection of electron momentum along the scattering vector direction.

$\Psi_0^c(K_n)$ is the Fourier transform of the RFA wave function $\phi_0^c(r)$.

(S_Electrons): The procedure for computing Compton profiles is already published and here we rewrite these equation for the sake of completeness. Following Berggren [17] the momentum transform of a Bloch function (for the unhybridised outermost “s” electrons) for the cubic structures is given by:

$$\Psi_{\vec{k}}(\vec{p}) = N\delta(\vec{p} - \vec{k}, \vec{k}_n)\Psi_{\vec{k}}^c(\vec{p}) \quad (3)$$

Here N is the total number of atoms, \vec{k}_n is the reciprocal lattice vector and the transform $\Psi_{\vec{k}}^c(\vec{p})$ is defined as:

$$\Psi_{\vec{k}}^c(\vec{p}) = (2\pi)^{-\frac{3}{2}} \int e^{-i\vec{p}\cdot\vec{r}} \Psi_{\vec{k}}(\vec{r}) d\vec{r} \quad (4)$$

Where the integration is over the Wigner-Seitz polyhedron .In the conventional cell approximation and the transform

$$\Psi_{\vec{k}}(\vec{r}) = e^{i\vec{k}\cdot\vec{r}} \Psi_{\vec{k}=0}(\vec{r}) \quad (5)$$

When $\vec{k}_n = \vec{p} - \vec{k}$, then $\vec{k} = 0$

$$\Psi_{\vec{k}}^c(\vec{p}) = \Psi_0^c(\vec{k}_n) \quad (6)$$

For $k_n = 0$

$$\Psi_0^c(0) = (2/\pi)^{\frac{1}{2}} \int_0^{r_0} dr r^2 \phi_0^c(r) \quad (7)$$

And for $k_n \neq 0$

$$\Psi_0^c(\vec{k}_n) = (2/\pi)^{\frac{1}{2}} k_n^{-1} \int_0^{r_0} dr r \sin(k_n r) [\phi_0^c(r) - \phi_0^c(r_0)] \quad (8)$$

The auxiliary function $G_n(p_n)$ is given as.

For $n = 0$

$$G_0(P_z) = \begin{cases} \frac{1}{2}(P_F^2 - P_z^2)P_z \leq P_F \\ 0 \text{ otherwise} \end{cases} \quad (9)$$

For $n \neq 0$

$$G_n(P_z) = \begin{cases} 0 & P_z > K_n + P_F \\ \tilde{G}_n(P_z)P_z \in (K_n - P_F, K_n + P_F) & \\ \tilde{G}_n(K_n - P_F)P_z < K_n - P_F & \end{cases} \quad (10)$$

Where

$$\tilde{G}_n(P_z) = \frac{N_n \{ (P_F^2 - K_n^2)(K_n + P_F - P_z) - \frac{1}{3}[(K_n + P_F)^3 - P_z^3] + K_n[(K_n + P_F)^2 - P_z^2] \}}{4K_n} \quad (11)$$

N_n is the number of reciprocal lattice points in the shell in the reciprocal space, as regards the wave function for 4s electrons, the free atom Hartree -Fock wave function was taken from tables of [18]. The Compton profile was then calculated using equation (2) to (6) for several cases choosing various (3d-4s) configuration. The Compton profile values of the of 3d shell and other inner shell electrons were taken from [19]. All the theoretical values were normalized to an area of 11.88267. As usual in all 15 shortest reciprocal lattice vectors were considered.

2-2 Free Electron-based model profile:

In case of an isotropic momentum distribution, equ (1) reduces to the well-known form:

$$J_{4s}(p_z) = 2\pi \int_{p_z}^{\infty} dp \rho(\vec{p}) p \quad (12)$$

If we consider the valence electrons in a metal as a non-interacting electron gas, then the momentum density by:

$$\rho(\vec{p}) = \text{constant} = \frac{n}{\frac{4}{3}\pi p_F^3} \quad (13)$$

Where n the number of free electrons per site and p_F is the Fermi momentum.

Substitution of $\rho(p)$ from eq.(13) to eq.(12) gives:

$$J_{4s}(p_z) = \frac{3n}{4p_F^3} (p_F^2 - p_z^2) \text{ for } p_z \leq p_F \quad (14)$$

The free electron Compton profile is then an inverted parabola including discontinuities of the first derivative at $\pm p_F$ [6]. Using eq.(14), we have also calculated the free electron Compton profile for 4s electron of Fe.

To get a total profile in the momentum range (0 to +6)a.u., the Compton profile for core electrons(1s² to 3d⁸) were directly taken from the tables of Biggs et al [20].

2-3 Cohesive energy:

The cohesive energy which is defined as the difference between the total ground -state energy of the solid and the energy of the individual isolated atoms can be calculated from Compton profile data [21] using following relation:

$$E_{\text{Coh}} = \int_0^{p_{\text{max}}} p_z^2 [J_s(p_z) - J_{\text{FA}}(p_z)] dp_z \quad (15)$$

Where the $J_s(p_z)$ and $J_{\text{FA}}(p_z)$ refer to solid state and free atom profiles, respectively. In our calculation, p_{max} was taken as infinite. The values of $J_s(p_z)$ were taken from the present RFA calculation which represents the solid-state phase of (Ni) and those for free atom Compton profile tables. The contribution core electrons are same in the $J_s(p_z)$ and $J_{\text{FA}}(p_z)$ and hence cancel out in the difference seen in Eq(15).

2-4 Band structure:

The one-electron band structure energy is given by[22]:

$$E_{\text{band}} = \sum_i \left(\int_{-\infty}^{E_f} E N_i(E) dE - \sum_{\alpha} n_{i,\alpha} \epsilon_{\alpha} \right) \quad (16)$$

Here, The summation extends over all atomic sites i , $N_i(E)$ is the local electronic density of states, and E_f is the Fermi energy which is a global quantity. The reference energy of an isolated atom is expressed in terms of the energy levels ϵ_{α} and the corresponding occupation numbers $n_{i,\alpha}$ which satisfy the condition.

$$\sum_{\alpha} n_{i,\alpha} = \int_{-\infty}^{E_f} N_i(E) dE \quad (17)$$

With this definition, E_{band} is zero for both empty and full bands.

In Fig (1), we show the band structure of a Ni (fcc) crystal as obtained by the (DFT-LDA) using code Quantum wise. And it was compared with the tight-binding and the ab initio LDA method [22]. We find that the agreement between these two calculations is very good, especially in the energy range close to the Fermi level E_f .

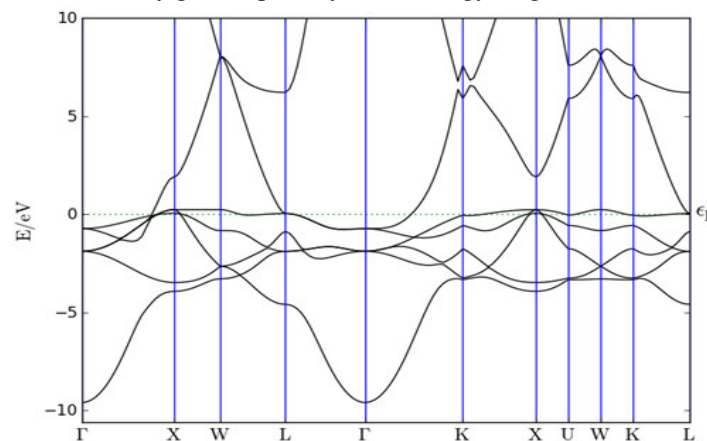


Figure 1. Band structure of Ni (fcc) obtained the (DFT-LDA) using code Quantum wise.

2-5 Density of state:

The magnetic interaction in this system can be obtained using the Stoner- theory of itinerant ferromagnetism[22]. This theory describes the electronic structure of the magnetic system by a rigid shift of the spin-up and spin-down states as.

$$N_{\uparrow}(E) = N(E + \Delta E_{\uparrow}) \quad (18)$$

$$N_{\downarrow}(E) = N(E - \Delta E_{\downarrow}) \quad (19)$$

Here, $N_{\uparrow}(E)$ and $N_{\downarrow}(E)$ are the densities of states for spin-up and spin-down electrons corresponding to majority and minority sub bands, respectively, and $N(E)$ is the density of states for the nonmagnetic state. The energy shifts ΔE_{\uparrow} and ΔE_{\downarrow} of $N_{\uparrow}(E)$ and $N_{\downarrow}(E)$ with respect to $N(E)$ are constrained by the charge conservation[22].

$$\int_{E_f - \Delta E_{\downarrow}}^{E_f} N(E) dE = \int_{E_f}^{E_f + \Delta E_{\uparrow}} N(E) dE \quad (20)$$

Our results for the corresponding total electronic density of states $N(E)$ of Ni (fcc) at displayed in Fig 2, again in very good agreement with each other. The density of states is dominated by a large peak near the Fermi level which is responsible for a stable ferromagnetic phase of Ni (fcc).

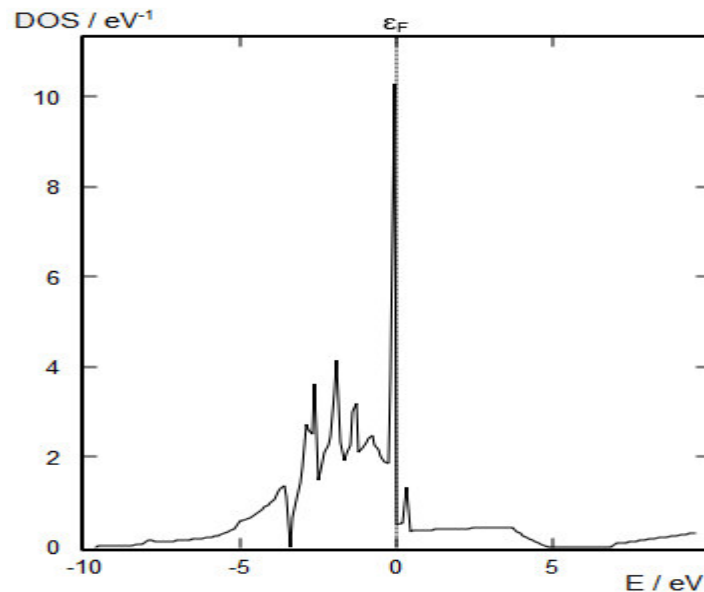


Figure 2 .Nonmagnetic density of states for Ni(fcc) obtained the(DFT-LDA) using code Quantum wise .

Results and Discussion

Table 1. Includes three theoretical profiles for $(3d^9-4s^1, 3d^{8.9}-4s^{1.1}, 3d^{8.8}-4s^{1.2})$ computed by RFA model using the procedure of Sec.2.A. The free atom values for $(3d^8-4s^2)$ are also included for comparison. Also given here are the Free electron profile .All the theoretical values given in this table I are obtained **after** convoluting the theory with the residual instrumental function (RIF) of 0.6 a.u. and normalized to an area of **11.88267** being the number of electrons form 0 to 6 a.u. Now we compare the various theoretical and experimental Compton profiles given in this table I . for the high momentum region ($p_z > 2.0$ a.u.), it is seen that all theoretical values are nearly equal, This is easily understood because in this region only core electron contribute to scattering process and for them the same model has been used in all cases. It is interesting to note that values are close to the experiment.

Coming next to the low momentum region ($p_z = 0-0.5$ a.u.) , it is seen that the free atom model shows the maximum disagreement. On the whole the RFA values are considerably flatter but the free electron values are close to the experiment. In Fig 3. shows this comparison where we plot the theoretical (except free atom) and experimental results upto 5 a.u. [20]. when ($p_z > 0.5$ a.u.) It is seen that the RFA values for $(3d^{8.8}-4s^{1.2})$ are lower than $(3d^9-4s^1, 3d^{8.9}-4s^{1.1})$ results but between ($p_z > 0.8$ a.u.) a.u. the trend is reversed and the $(3d^{8.8}-4s^{1.2})$ values are higher than from $(d^9-4s^1, 3d^{8.9}-4s^{1.1})$.

Comparison between Free electron and Free atom, it is seen in low momentum Free atom $(3d^8-4s^2)$ higher than the Free electron $(3d^8-4s^2)$ but in part between $p_z = (0.3$ and $0.8)$ the trends get reversed and the free electron values are somewhat larger than the free atom . At $p_z > 0.9$ a.u. both models values to become similar. In Fig(4) shows the difference between theoretical (after convolution) and experimental profiles in Fe. It can be seen in the low momentum that $\Delta J(3d^9-4s^1, 3d^{8.9}-4s^{1.1} - \text{Exp})$ larger than from $\Delta J(3d^{8.8}-4s^{1.2} - \text{Exp})$, as well as the $\Delta J(3d^{8.8}-4s^{1.2} - \text{Exp})$, have similar values only in low momentum different, but (Free atom - Expt and Free Electron - Expt) are nearly the same where $p_z > 1$ a.u. Also in the high momentum transfer region ($p_z > 4$ a.u.) , Experimental values are very close to corresponding theoretical data. It is known that the contribution of valence electron is very small in this region and hence, most of the contribution may be due to the inner-core electrons. These inner-core electrons are reasonably described by the free-atom values. In order to determine the best configuration electrons, the total square deviation $\sum_0^{6 \text{ a.u.}} |\Delta J|^2$ was obtained for each cases . The values founded were **(0.3001139, 0.292883, 0 .292636)** for $(3d^9-4s^1, 3d^{8.9}-4s^{1.1}, 3d^{8.8}-4s^{1.2})$ configuration respectively. Thus $(3d^{8.8}-4s^{1.2})$ seems to be the best configuration. From this we can observe by effect of convolution the theoretical values. The purpose of the computation of cohesive energy was to see the applicability of the RFA scheme in reproducing the cohesive of transition metals. The value of calculated cohesive energy (with $p_{\text{max}} = 2$ a.u.). Table 2. Show comparison between our theoretical by RFA model, experiment [20] and another data. A choice of low value of p_{max} is justified because, to a good approximation ,after this value the major contribution in the theoretical and experimental profile is expected only due to core electrons, which almost remain. unaffected in formation of solids.

Table 1: Theoretical results Compton profile of Nickel (Ni) compared with experimental value [20]. All the quantities in atomic units .All theoretical values have been convoluted with the residual instrumental function (RIF) of 0.6 a.u. These values have been normalized to 11.88267 electrons as discussed in the text.

P_z (a.u.)	$J(p_z)(e/a.u.)$					
	Free atom ($3d^8-4s^2$)	Free electron ($3d^9-4s^1$)	Theory(RFA)			Expt. [20]
			Core +RFA $3d^9-4s^1$	Core +RFA $3d^{8.9}-4s^{1.1}$	Core +RFA $3d^{8.8}-4s^{1.2}$	
0.0	6.720	5.383	5.232	5.208	5.192	5.18
0.1	6.357	5.313	5.175	5.156	5.143	5.17
0.2	5.915	5.211	5.089	5.075	5.066	5.11
0.3	5.511	5.082	4.98	4.973	4.969	5.03
0.4	5.145	4.928	4.853	4.852	4.853	4.92
0.5	4.807	4.752	4.705	4.708	4.714	4.77
0.6	4.506	4.563	4.543	4.55	4.558	4.6
0.7	4.255	4.373	4.379	4.387	4.395	4.42
0.8	4.053	4.195	4.223	4.228	4.236	4.24
1.0	3.756	3.890	3.944	3.944	3.948	3.89
1.2	3.512	3.632	3.691	3.689	3.689	3.55
1.4	3.264	3.377	3.431	3.428	3.428	3.22
1.6	3.000	3.109	3.156	3.153	3.153	2.91
1.8	2.729	2.836	2.874	2.871	2.871	2.63
2	2.465	2.566	2.596	2.594	2.594	2.36
3	1.435	1.493	1.504	1.504	1.504	1.38
4	0.894	0.925	0.932	0.933	0.934	0.87
5	0.643	0.660	0.665	0.666	0.667	0.53

Table 2: Cohesive energy of Nickel. (E_{coh} (in eV)

Reference	E_{coh} (in eV)
Our theoretical(RFA)	4.97
Experiment[21]	4.44

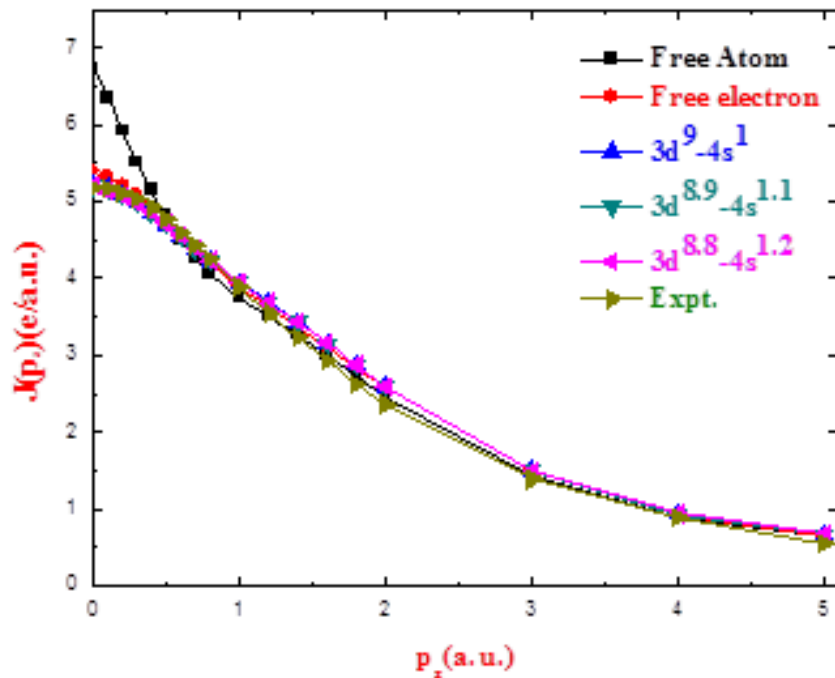


Fig 3: Comparison of theoretical results with experimental [20] Compton profiles for Ni.

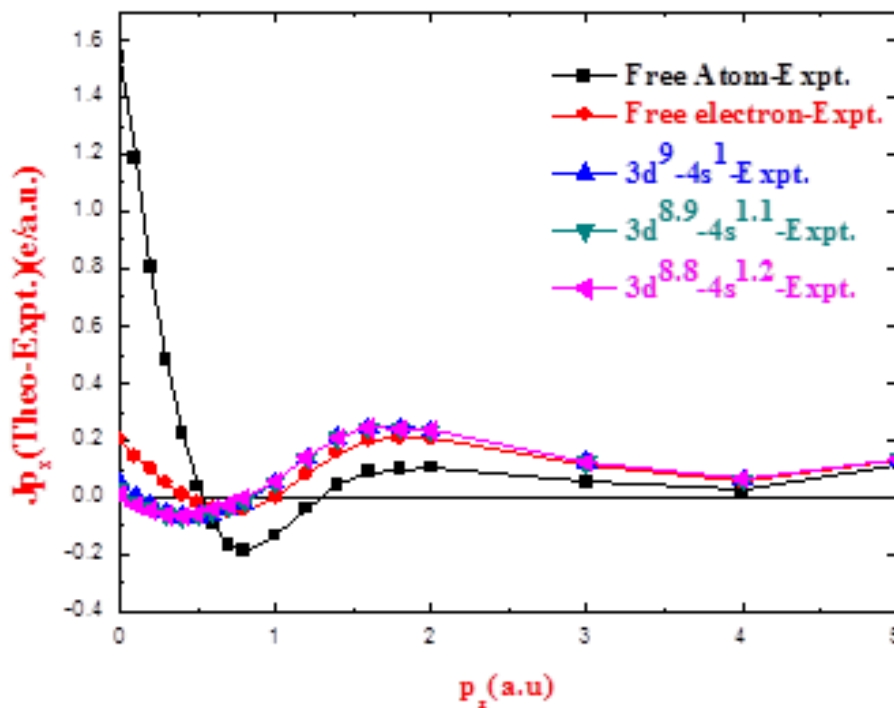


Fig 4: Difference between our theoretical and experimental [20] Compton profiles of Ni.

Conclusion

The RFA model shows good agreement with the experiment in the $(3d^{8.8}-4s^{1.2})$ configuration, while free electron model are higher than experimental. Evidently, there is a need for a relativistic band structure calculation to interpret the Compton profile data. In table I illustrate the comparison between theoretical results using (RFA) model with previous works [20] in the process transfer charge of shells (s,d). The cohesive energy of Nickel computed by (RFA) model and comparison with another results [20].

References

1. Heubner, U., (1998) "Nickel Alloys" Marcel Dekker, Inc., ISBN0-8247-0440-1.
2. Pearson, W.B. "A handbook of lattice spacing and structure of metals and alloys" (1964), (New York: Pergamon press).
3. Paakkari, T. Manninen, S. and Berggren, K.F. (1975) Phys. Fenn. 10207.
4. Berggren, F.K. Manninen, S. Paakkari, T. Aikala, O and Mansikka, K. (1977) Compton scattering (ed.) B.G. Williams (New York: McGrawHill).
5. Sharma, B.K., Singh, H., Perkkiö, S., Paakkari, T. and Mansikka, K. (1986) Report Ser. Turku FTL-R109 Finland, (also 1987 Phys. Status Solidi B141 177).
6. Sharma, B.K., Gupta, A., Singh, H., Perkkiö, S., Kshirsagar, A. and Kanhere, D.G. (1988) Phys. Rev. B37 6821
7. Gupta, A., Singh, H. and Sharma, B.K. (1988), Nucl. Solid state Phys. Symp C26 212..
8. V. Sundararajan, R. Asokamani and D. G. Kanhere. *Phys. Rev. B* 38, 12653 (1988).
9. A. R. Jani, G. S. Tripathi, N. E. Brener and J. Callaway. *Phys. Rev. B* 40, 1593 (1989).
10. N. Munjal, P. Bhambhani, V. Vays, P. Ahmad, G. Sharma, B. K. Sharma. *World Journal of Condensed Matter Physics*, 1, pp (70-76), 13012 (2011).
11. Patte, P., Manninen, S. and Paakkari, T. Deconvolution in Compton Profile Measurement, *phil. Mag.* 30, 1281, (1974).
12. Cooper, M. J. (1985). *Rep. Prog. Phys.* 48, 415.
13. Andrejczuk, A. Reniewicz, H. Dobrzyuski, L. Zukowski, E. and Kaprzyk, S. (2000). *Phys. Status Solidi B* 217, 903.
14. Chodorow, M. (1939), *Phys. Rev.* 55, 675.
15. Berggren, K.F., Manninen, S. and Paakkari, T. (1973). *Phys. Rev.* B55 2516.
16. Berggren, K.F. (1972), *Phys. Rev.* B6 2156-61.
17. Clementi, E. and Roetti, C. (1974). *Atomic Data and Nucl. Data Tables* 14 212.
18. Bigges, L., Mendelsohn, L., Bandmann, J.B. (1975). *At. Data Nucl. Data Tables* 16, 201.
19. Holt, R. S. and Cooper, M.J. (1980) "The calculation of electronic energies from Compton Profiles". *Philos. Mag.* B 41 (2), 117-121.
20. B. L. Ahuja, M. D. Sharma, B. K. Sharma, S. Hamouda and M. J. Cooper. (1998). "Compton Study of the Electronic State in Fe-Ni Alloys" *Physica Scripta*. Vol. 58, 185-188
21. Calculating the Cohesive Energy of Rare Gas Solids." *Journal of Chemical Education*, volume 89, number 5, 2012, pp. 592-597.
22. W. Zhong, G. Overney, and D. Tomanek, (1993) "Structural properties of Fe crystals". *Phys. Rev. B* 47, 95